
PERGAMON

Journal of Quantitative Spectroscopy & Radiative Transfer 79–80 (2003) 533–547

Journal of Quantitative Spectroscopy & Radiative Transfer

www.elsevier.com/locate/jqsrt

A recursive centered T-matrix algorithm to solve the multiple scattering equation: numerical validation

Jean-Claude Auger[a,*], Brian Stout[b]

[a] *Centro de Investigación en Polímeros, Grupo COMEX, Blv M. A. Camacho No 138, Lomas de Chapultepec, 11560 México D.F, Mexico*

[b] *Institut Fresnel UMR 6133, Faculté des Sciences et Techniques, Centre de Saint Jeróme, Marseilles Cedex 20 13397, France*

Received 10 July 2002; received in revised form 1 October 2002; accepted 2 October 2002

Abstract

The multiple scattering problem can be solved using various analytical techniques. One of these techniques, the T-matrix formalism, is at the present time generally solved using iterative algorithms, because the initially proposed recursive algorithms appeared to be numerically unstable. We present here a new set of recursive relations to solve the multiple scattering equation, and discuss their range of application. In order to validate this new formalism, we compare numerical results for various complex systems with the Generalized Multi-particle Mie solution. We show that the results obtained with the recursive method are in very good agreement with those given by iterative techniques.

Keywords: Multiple-scattering; T-matrix; Recursive algorithm

1. Introduction

Theoretical and experimental studies of multiple light scattering by a collection of particles have a large scientific interest in academic research as well as in the industry. Some of its numerous applications are in astrophysics and atmospheric sciences, but one also finds applications in the ink or coating industries where one strives to optimize tinting strength and hiding power. Although multiple scattering theory has been investigated since the end of the 1960s [1,2], the complexity of the formalism has limited the range of applications.

* Corresponding author. Tel.: +52-594-95-71602; fax: +52-594-95-71604.
E-mail address: jcauger@cip.org (J.-C. Auger).

0022-4073/03/$ - see front matter
doi:10.1016/S0022-4073(02)00306-0

Since the arrival of new computer capabilities, this field of research has seen considerable developments. The aim of multiple scattering calculations is to evaluate the total electromagnetic field which results from the interaction of an incident wave with a multitude of particles embedded in a homogeneous medium. The radiative transfer equation [3,4] is an elegant way to formulate this problem which also permits one to easily introduce the boundary condition at the propagation medium interfaces. Nevertheless, the range of applications of this technique is limited due to the fact that the calculations are performed on the intensities of the fields and not the fields themselves. For a dense collection of particles, the formalism fails because interference effects become non-negligible and one has to perform the calculations on the vector fields. Among the various analytical techniques used to solve the vectorial multiple scattering equation, the Green's tensor and the T-matrix approaches are widely used [5]. The first approach is a direct resolution of the integral equation of the electric and magnetic fields using the Green's tensor. The total field can be evaluated through a statistical formalism which considers a radial pair correlation function of the particles instead of specifying each of their positions in the medium [6,7]. The second approach is based on the T-matrix formalism coupled with the Extended Boundary Condition techniques (EBC), also called the Null Field Approach introduced by Watermann [8] for an isolated particle. The electro-magnetic fields are expanded on the Vectorial Spherical Wave (VSW) basis and the expansion coefficients of the scattered and incident field are linked by a single matrix usually called T-matrix. Its coefficients are related to surface integrals of the electromagnetic fields on the particle's interface, and they simplify greatly for spherical scatterer geometries. The T-matrix depends on the nature, size and shape of the particle, as well as the wavelength of the incident radiation. The T-matrix formalism can also be extended to the multiple scattering problem. A multiple T-matrix is associated to each particle of the system. It is characterized by the optical properties of the particle and takes into account the presence of all the other scatters. The multiple scattering equations lead to a linear system of N coupled equations, where N is the total number of particles. The unknowns are the scattering field's coefficients or the multiple T-matrices. Due to the ill-conditioned state of the general matrix, the linear system cannot be numerically solved by direct inversion techniques. To overcome this problem, various alternative techniques were proposed such as iterative algorithms [9–11,13,15,16] or recursive processes [12,14]. In all these studies, the authors considered either dielectric or metallic spherical particles embedded in an infinite homogeneous non absorbing medium. However, if iterative algorithms have shown to be successful, it seems that the recursive procedure proposed by Chew and Tzeng introduce large numerical errors. An alternative recursive algorithm has been recently proposed [17,18]. This algorithm is based on the Recursive T-matrix Algorithm (RTMA) developed by Chew, and the Centered T-matrix concept introduced by Mackowski [19]. For this reason, we will refer to it in this study as the Recursive Centered T-Matrix Algorithm (RCTMA).

The aim of this work is to point out some of the main possibilities of this new formalism. Also, in order to validate this new technique, we evaluate and compare numerical calculations of the optical parameters of various systems with the results obtained by an iterative algorithm. The article is organized as follows : Section 2 gives a brief review of the multiple scattering formalism using the T-matrix method, and the expansion of the electromagnetic fields on the vectorial spherical waves basis. Section 3 focuses on the derivation and validity of the original recursive algorithms, while in Section 4 we develop and comment on the new recursive relations. Section 5 is devoted to the comparative studies with the Generalized Multiparticle Mie-solution (GMM) [20].

2. General T-matrix representation of the multiple scattering equation

We consider a monochromatic plane wave of wave vector $\mathbf{k}_{\text{inc}}$ and frequency ω impinging on a dielectric spherical particle with a complex index of refraction n_s and radius a, embedded in an infinite non-absorbing medium of index of refraction n_0. The incident and scattered fields, $\mathbf{E}_{\text{inc}}$ and $\mathbf{E}_{\text{sca}}$ can be expanded on the vectorial spherical waves basis $Rg\{\mathbf{\Psi}\}$ and $\mathbf{\Psi}(k_{\text{inc}}\mathbf{r})$ [21] such as

$$\mathbf{E}_{\text{inc}} = Rg\{\mathbf{\Psi}^{\text{t}}(k_{\text{inc}}\mathbf{r})\} \cdot \mathbf{a}, \tag{1}$$

$$\mathbf{E}_{\text{sca}} = \mathbf{\Psi}^{\text{t}}(k_{\text{inc}}\mathbf{r}) \cdot \mathbf{f}, \tag{2}$$

where $\mathbf{a}$ and $\mathbf{f}$ are column vectors representing the incident and scattered field expansion coefficients. Rg stands for the regular part (non-singular at the origin) while the superscript t stands for the transpose.

Using the T-matrix formalism, $\mathbf{a}$ and $\mathbf{f}$ can be linked through the relation $\mathbf{f} = \mathbf{T}^{1(1)} \cdot \mathbf{a}$ [8], where $\mathbf{T}^{1(1)}$ is the single T-matrix of the particle. Let us consider now a collection of N randomly located spheres with radius a_i and complex refractive indexes n_s^i $(i = 1, N)$. The center of each sphere O_i is defined in a principal coordinate system O by position vectors $\mathbf{r}_i$ and the relative position vector between two arbitrary spheres i and j is denoted by $\mathbf{r}_{ij}$. The excitation field $\mathbf{E}_{\text{exc}}^{i(N)}$ is defined as the total external field impinging on the ith sphere. In the multiple scattering formalism, it is the sum of the applied incident field $\mathbf{E}_{\text{inc}}$ and the fields $\mathbf{E}_{\text{sca}}^{j(N)}$ scattered by all the other spheres. As in the single particle theory, the electromagnetic fields are expanded in terms of spherical vector wave functions. However, while the incident field is naturally expanded in the principal coordinate system O, the fields scattered from each of the jth spheres are expanded in the coordinate systems O_j. Therefore, in order to express both terms in the coordinate system of the ith sphere, one should use the translational addition theorem [22] (Eqs. (A.1) and (A.2)). The analytical expression of the excitation field is then given by

$$\mathbf{E}_{\text{exc}}^{i(N)} = Rg\{\mathbf{\Psi}^{\text{t}}(k_{\text{inc}}\,|\mathbf{r} - \mathbf{r}_i|)\} \cdot \bar{\mathbf{J}}^{(i,0)} \cdot \mathbf{a} + \sum_{\substack{j=1 \\ j\neq i}}^{N} Rg\{\mathbf{\Psi}^{\text{t}}(k_{\text{inc}}\,|\mathbf{r} - \mathbf{r}_i|)\} \cdot \bar{\mathbf{H}}^{(i,j)} \cdot \mathbf{f}^{j(N)}, \quad i = 1, \ldots, N, \tag{3}$$

where $\mathbf{f}^{j(N)}$ is the column vector representing the expansion coefficients of the scattered field by the jth particle. The $\bar{\mathbf{J}}^{(i,0)}$ and $\bar{\mathbf{H}}^{(i,j)}$ represent the translational matrices defined in Eq. (A.4). Combining the single T-matrix's relation with the expression of the excited field Eq. (3) yields a linear system of N coupled equations

$$\mathbf{f}^{i(N)} = \bar{\mathbf{T}}^{i(1)} \cdot \left[\bar{\mathbf{J}}^{(i,0)} \cdot \mathbf{a} + \sum_{\substack{j=1 \\ j\neq i}}^{N} \bar{\mathbf{H}}^{(i,j)} \cdot \mathbf{f}^{j(N)} \right], \quad i = 1, \ldots, N. \tag{4}$$

Introducing the multiple T-matrix $\bar{\mathbf{T}}^{i(N)}$ of the ith sphere, each scattered field can be directly linked to the incident field coefficients through the relation

$$\mathbf{f}^{i(N)} = \bar{\mathbf{T}}^{i(N)} \cdot \bar{\mathbf{J}}^{(i,0)} \cdot \mathbf{a}, \quad i = 1, \ldots, N. \tag{5}$$

We remark that the matrix $\bar{\mathbf{T}}^{i(N)}$ is independent of the orientation or polarization of the incident wave, and that it characterizes the scattering properties of the ith particle while taking into account the presence of the others. Inserting Eq. (5) into Eq. (4) yields a new linear system of coupled equations where the unknowns are now the multiple T-matrices

$$\bar{\mathbf{T}}^{i(N)} \cdot \bar{\mathbf{J}}^{(i,0)} = \bar{\mathbf{T}}^{i(1)} \cdot \left[\bar{\mathbf{J}}^{(i,0)} + \sum_{\substack{j=1 \\ j \neq i}}^{N} \bar{\mathbf{H}}^{(i,j)} \cdot \bar{\mathbf{T}}^{j(N)} \cdot \bar{\mathbf{J}}^{(j,0)} \right], \quad i = 1, \ldots, N. \tag{6}$$

Eqs. (4) and (6) are generally solved by an iterative algorithm. Directly solving Eq. (4) is numerically faster, but the solutions of the fields are only valid for the specified orientation of the incident wave. However, since the multiple T-matrices are independent of the incident field's orientation, solving Eq. (6), allows a complete characterization of the system for any orientation. Moreover, the knowledge of the $\bar{\mathbf{T}}^{i(N)}$ matrices allows one to derive the average optical parameters of the system, where the average is realized over all possible directions of incidence, and polarizations of the incident field.

The multiple T-matrices of Eq. (6) can also be solved through a recursive formalism that was first introduced by Chew for scalar waves [12]. Later, Tzeng extended this formalism to electromagnetic fields [14]. The purpose of the next section is to present the derivation of those recursive algorithms.

3. Recursive solution to the multiple scattering equation

We consider a system composed of $N-1$ particles whose multiple T-matrices $\bar{\mathbf{T}}^{i(N-1)}$ are all known. An Nth sphere is added to the system, and placed farthest from the origin of the principal coordinate system. Using Eq. (6) its multiple T-matrix $\bar{\mathbf{T}}^{N(N)}$ can be expressed as

$$\bar{\mathbf{T}}^{N(N)} \cdot \bar{\mathbf{J}}^{(N,0)} = \bar{\mathbf{T}}^{N(1)} \cdot \left[\bar{\mathbf{J}}^{(N,0)} + \sum_{i=1}^{N-1} \bar{\mathbf{H}}^{(N,i)} \cdot \bar{\mathbf{T}}^{i(N)} \cdot \bar{\mathbf{J}}^{(i,0)} \right]. \tag{7}$$

Now considering the $\bar{\mathbf{T}}^{i(N-1)}$ matrix of the ith remaining particle as an effective single T-matrix, the corresponding excited fields are the sum of the incident and the scattered fields of the Nth particle. In terms of multiple T-matrix relation, this gives

$$\bar{\mathbf{T}}^{i(N)} \cdot \bar{\mathbf{J}}^{(i,0)} = \bar{\mathbf{T}}^{i(N-1)} \cdot [\bar{\mathbf{J}}^{(i,0)} + \bar{\mathbf{H}}^{(i,N)} \cdot \bar{\mathbf{T}}^{N(N)} \cdot \bar{\mathbf{J}}^{(N,0)}] \quad i \leqslant N-1. \tag{8}$$

In order to solve the $\bar{\mathbf{T}}^{i(N)}$ matrices, the expression of $\bar{\mathbf{T}}^{i(N)} \cdot \bar{\mathbf{J}}^{(i,0)}$ of Eq. (8) is used in Eq. (7). After some algebra, one finds:

$$\bar{\mathbf{T}}^{N(N)} \cdot \bar{\mathbf{J}}^{(N,0)} = \left[\mathbf{I} - \bar{\mathbf{T}}^{N(1)} \sum_{i=1}^{N-1} \bar{\mathbf{H}}^{(N,i)} \cdot \bar{\mathbf{T}}^{i(N-1)} \cdot \bar{\mathbf{J}}^{(i,0)} \cdot \bar{\mathbf{H}}^{(0,N)} \right]^{-1}$$

$$\bar{\mathbf{T}}^{N(1)} \cdot \left[\bar{\mathbf{J}}^{(N,0)} + \sum_{i=1}^{N-1} \bar{\mathbf{H}}^{(N,i)} \cdot \bar{\mathbf{T}}^{i(N-1)} \cdot \bar{\mathbf{J}}^{(i,0)} \right], \tag{9}$$

$$\bar{\mathbf{T}}^{i(N)} \cdot \bar{\mathbf{J}}^{(i,0)} = \bar{\mathbf{T}}^{i(N-1)} \cdot \bar{\mathbf{J}}^{(i,0)} \cdot [\mathbf{I} + \bar{\mathbf{H}}^{(0,N)} \cdot \bar{\mathbf{T}}^{N(N)} \cdot \bar{\mathbf{J}}^{(N,0)}] \quad i \leqslant N-1. \tag{10}$$

Eqs. (9) and (10) are the recursive relations of the Recursive T-Matrix Algorithm (RTMA). This algorithm has two steps: first, one needs to evaluate the multiple T-matrix $\bar{\mathbf{T}}^{N(N)}$ of the Nth scatterer as a function of the $\bar{\mathbf{T}}^{i(N-1)}$ matrices of each constituent of the $(N-1)$ cluster Eq. (9). Then, the individual multiple-scattering T-matrices $\bar{\mathbf{T}}^{i(N)}$ for a cluster with N scatterers are evaluated from the previous individual multiple-scattering T-matrices $\bar{\mathbf{T}}^{i(N-1)}$ and the $\bar{\mathbf{T}}^{N(N)}$ matrix via Eq. (10). Using the superposition principle of electromagnetic waves, one can express the total scattered field of the whole system. However as each scattered field is expanded in a different basis, one needs to translate them into a common coordinate system. Using Eq. (A.3) of the translational theorem, the expansion coefficients of the total scattered field $\mathbf{f}^{T(N)}$ can be expressed as $\mathbf{f}^{T(N)} = \sum_{i=1}^{N} \bar{\mathbf{J}}^{(0,i)} \cdot \mathbf{f}^{i(N)}$. In terms of multiple T-matrices it gives

$$\mathbf{f}^{T(N)} = \sum_{i=1}^{N} \bar{\mathbf{J}}^{(0,i)} \cdot \bar{\mathbf{T}}^{i(N)} \cdot \bar{\mathbf{J}}^{(i,0)} \cdot \mathbf{a} = \bar{\mathbf{T}}^{T(N)} \cdot \mathbf{a}, \tag{11}$$

where $\bar{\mathbf{T}}^{T(N)}$ is the total T-matrix of the system. Once evaluated, the system can be treated as a single arbitrarily shaped particle.

Now, inserting the expression $\bar{\mathbf{T}}^{T(N)}$ of Eq. (11) into the recursive relations of the RTMA yields:

$$\bar{\mathbf{T}}^{N(N)} \cdot \bar{\mathbf{J}}^{(N,0)} = [\mathbf{I} - \bar{\mathbf{T}}^{N(1)} \bar{\mathbf{H}}^{(N,0)} \cdot \bar{\mathbf{T}}^{T(N-1)} \cdot \bar{\mathbf{H}}^{(0,N)}]^{-1}$$

$$\bar{\mathbf{T}}^{N(1)} \cdot [\bar{\mathbf{J}}^{(N,0)} + \bar{\mathbf{H}}^{(N,0)} \cdot \bar{\mathbf{T}}^{T(N-1)}], \tag{12}$$

$$\bar{\mathbf{T}}^{T(N)} = \bar{\mathbf{T}}^{T(N-1)} \cdot [\bar{\mathbf{J}}^{(0,N)} + \bar{\mathbf{T}}^{T(N-1)} \cdot \bar{\mathbf{H}}^{(0,N)}] \bar{\mathbf{T}}^{N(N)} \cdot \bar{\mathbf{J}}^{(N,0)}. \tag{13}$$

Eqs. (12) and (13) define a new set of recursive relations known as Recursive Aggregate T-matrix Algorithm (RATMA) [12]. The total T-matrix of the N particles' system is calculated from the knowledge of the total T-matrix of the $N-1$ particles' system and the multiple T-matrix of the Nth sphere. It would then appear that the RTMA and RATMA are theoretically useful techniques to solve the multiple scattering equation. However, it is now well known that neither algorithm is numerically stable. In the next paragraph, we propose to discuss the causes of their numerical instability. It turns out that even if one assumes that the series expansions of the translation addition

theorem are uniformly convergent, for the computation of the N-spheres problem, the stability of the recursive algorithms can be compromised.

We recall that the T-matrix formalism involves an infinite expansion of the electric and magnetic fields on the partial spherical wave basis. The incident field is expressed therefore as an infinite superposition of partial spherical waves. The total scattering process is then the summation of the individual scattering interactions between each partial spherical waves and the particle. However, the radial behavior of the different partial waves vary with their corresponding order n. For this reason, there exists a maximum order $n_{\max}$ beyond which the partial waves of superior order $n > n_{\max}$ will not have a physical interaction with the particle [23]. Thereafter, the infinite series expansion of the electromagnetic fields can be simply truncated at the order $n_{\max}$ where they certainly converge. This order of truncation depends on the size parameter of the particle. It is usually admitted that Wiscombe's criterion allows for an accurate determination of its value [24].

The $\bar{\mathbf{H}}^{(i,j)}$ matrices describe the continuity of the tangential components of all scattered electric fields across each surface of the ith sphere. Since they do not need to describe more partial waves than those which are effectively interacting with the particle, the infinite series expansions given by Eq. (A.2) can also be truncated at the order $n_{\max}$. Then, the dimensions of the $\bar{\mathbf{H}}^{(i,j)}$ matrices only depends on the size parameter of the particles and are equal to $d_n \times d_n$, where $d_n = 2n_{\max}(n_{\max}+2)$.

The RTMA and RATMA techniques also involve the translation matrices $\bar{\mathbf{J}}^{(i,0)}$ and $\bar{\mathbf{J}}^{(0,i)}$. However, even if they have the same analytical expression as given in Eq. (A.4), they play a different physical role. The $\bar{\mathbf{J}}^{(i,0)}$ matrices are used to translate a monochromatic plane wave coefficients $\mathbf{a}$ from the principal coordinate system to the ith basis (Eq. (A.1)). But, as the expansion coefficients of a plane wave on the spherical basis never vanish, the necessary cut-off of the infinite series Eq. (A.1) has to be done at an order $v_{\max}$ such as, $v_{\max} \gg n_{\max}$. The $\bar{\mathbf{J}}^{(i,0)}$ matrices must then be rectangular with dimensions $d_n \times d_v$, where $d_v = 2v_{\max}(v_{\max}+2)$.

In the formulation of the total T-matrix above, the $\bar{\mathbf{J}}^{(0,i)}$ matrices are used to translate the scattered fields $\mathbf{f}^{i(N)}$ from the basis of the ith particle to the principal coordinate system. However, in this description, the whole system is treated as a single particle, and the series expansions given by Eq. (A.3) have to be truncated at an order which depends now on the size parameter of the whole system. The $\bar{\mathbf{J}}^{(0,i)}$ matrices are likewise rectangular with dimensions $d_v \times d_n$. The fact that $v_{\max}$ is necessarily finite and relatively small in order to perform realistic numerical calculations will therefore compromise the numerical stability of the RTMA and RATMA techniques. Moreover, in order to express the term $\bar{\mathbf{T}}^{i(N-1)} \cdot \bar{\mathbf{J}}^{(i,0)}$ in Eq. (9), it was necessary to use a fundamental group relations between translational matrices of the type $\bar{\mathbf{H}}^{(i,N)} = \bar{\mathbf{J}}^{(i,0)} \cdot \bar{\mathbf{H}}^{(0,N)}$. This relation is only true in the theoretical case of infinite dimensions of the translation matrices. Since this is not the case during numerical simulations on computers, replacing $\bar{\mathbf{H}}^{(i,N)}$ by the product of finite dimensional matrices $\bar{\mathbf{J}}^{(i,0)} \cdot \bar{\mathbf{H}}^{(0,N)}$ will generate a numerical error.

Finally, in the total T-matrix representation, the total scattered field $\mathbf{f}^{T(N)}$ from Eq. (11) is only valid outside of the space occupied by the particles. The evaluation of the multiple T-matrix $\bar{\mathbf{T}}^{N(N)}\bar{\mathbf{J}}^{(N,0)}$ is not performed via a direct interaction taking into account the local field between the Nth and all the remaining ith particles. In conclusion, the fact that both algorithms involve the $\bar{\mathbf{J}}^{(i,0)}$ and $\bar{\mathbf{J}}^{(0,i)}$ matrices in their right and left hand sides can seriously degrade their numerical accuracy.

4. Recursive centered T-matrix algorithm

In order to cope with the numerical instabilities of the RTMA and RATMA formalisms, we proposed a new set of recursive relations based on the N-centered T-matrix concept $\bar{\tau}_N^{(i,j)}$. Mackowski [13], pointed out that the N-scattered T-matrix $\bar{\mathbf{T}}^{i(N)}$ of the ith sphere could be expressed in terms of the N-centered T-matrix $\bar{\tau}_N^{(i,j)}$ via the relation:

$$\bar{\mathbf{T}}^{i(N)} = \sum_{j=1}^{N} \bar{\tau}_N^{(i,j)} \cdot \bar{\mathbf{J}}^{(j,i)} \quad i = 1, \ldots, N. \tag{14}$$

Since the scattering properties of the cluster are given by the $\bar{\mathbf{T}}^{i(N)}$, these properties will be then fully specified once all the N-centered T-matrix $\bar{\tau}_N^{(i,j)}$ are determined. Introducing Eq. (14) into Eq. (9) and Eq. (10) leads to the following new set of four recursive equations. The recurrence relation involving $\bar{\mathbf{T}}^{N(N)}$ (i.e. Eq. (9)) gives rise to

$$\bar{\tau}_N^{(N,N)} = \left[\mathbf{I} - \bar{\mathbf{T}}^{N(1)} \cdot \sum_{i=1}^{N-1} \bar{\mathbf{H}}^{(N,i)} \cdot \sum_{j=1}^{N-1} \bar{\tau}_{N-1}^{(i,j)} \cdot \bar{\mathbf{H}}^{(j,N)} \right]^{-1} \cdot \bar{\mathbf{T}}^{N(1)} \tag{15}$$

$$\bar{\tau}_N^{(N,j)} = \bar{\tau}_N^{(N,N)} \cdot \sum_{i=1}^{N-1} \bar{\mathbf{H}}^{(N,i)} \cdot \bar{\tau}_{N-1}^{(i,j)}, \quad j \neq N. \tag{16}$$

Similarly, Eq. (10) involving the $\bar{\mathbf{T}}^{k(N)}$ matrices, $k = 1, \ldots, N-1$ yields:

$$\bar{\tau}_N^{(k,i)} = \bar{\tau}_{N-1}^{(k,i)} + \sum_{j=1}^{N-1} \bar{\tau}_{N-1}^{(k,j)} \cdot \bar{\mathbf{H}}^{(j,N)} \cdot \bar{\tau}_N^{(N,i)}, \quad i \neq N, \tag{17}$$

$$\bar{\tau}_N^{(k,N)} = \sum_{j=1}^{N-1} \bar{\tau}_{N-1}^{(k,j)} \cdot \bar{\mathbf{H}}^{(j,N)} \cdot \bar{\tau}_N^{(N,N)}, \quad i = N. \tag{18}$$

For simplicity, we refer to the above recursive relation as the Recursive Centered T-Matrix Algorithm (RCTMA). A complete and detailed derivation of this algorithm has been previously presented [17,18] and the reader is invited to consult the corresponding references for more informations. In the next paragraph, how and why this new set of recursive relations can lead to a stable accurate solution of the multiple scattering equation is explained.

Taking into account the discussion of the previous section, and examining Eqs. (15)–(18), one can make the following comments. The recursive relations are now directly based on the evaluation of the N-centered T-matrices themselves, and the only translation matrices involved are of the type $\bar{\mathbf{H}}^{(i,j)}$. We saw earlier that these infinite dimensional matrices can be reliably truncated at the same order as individual transfer matrices, without generating convergence errors. Also, each $\bar{\tau}_N^{(i,j)}$ matrices start with an ordinary one-particle transfer matrix of type $\bar{\mathbf{T}}^{i(1)}$, and end with a transfer matrix of type $\bar{\mathbf{T}}^{j(1)}$. These transfer matrices are thus naturally truncated by these matrices. The algorithm is then free from the convergence problem due to the presence of the $\bar{\mathbf{J}}^{(0,i)}$ and $\bar{\mathbf{J}}^{(i,0)}$ matrices, and the

truncation order only depends on the size parameter of the spheres. Furthermore, the total T-matrix of the system is never evaluated, and the solutions of the fields are not restricted to the space outside of the system, and one can evaluate the external and internal field of each of the particles throughout the entire space.

Once evaluated the N-centered T-matrix, one can calculate the optical parameters of the whole system such as the total cross section and the coefficients of the amplitude scattering matrix. Fuller [25] then Mackowski [13] derived a complete formalism in order to calculate those optical parameters directly from the N-multiple T-matrices. In this formalism, the total cross-sections are the sum of the individual cross-sections calculated on each sphere of the system. However, in order to evaluate the optical parameters for a fixed orientation of the incident field, one has to calculate the scattering fields coefficients given by Eq. (5).

Using the N-centered T-matrix representation one finds $\mathbf{f}^{i(N)} = \sum_{j=1}^{N} \bar{\boldsymbol{\tau}}_N^{(i,j)} \cdot \bar{\mathbf{J}}^{(j,0)} \cdot \mathbf{a}$. In this relation, one can see that the numerical evaluation of the expansion's coefficients of the scattered fields depends on the order of convergence of the $\bar{\mathbf{J}}^{(j,0)}$ matrices. To circumvent this difficulty Lo [26] and Bruning [27,28] replaced the $\bar{\mathbf{J}}^{(j,0)}$ matrices in the far field region by a phase shift term. Using this approach, the analytical expression of the expansion coefficients $\mathbf{f}^{i(N)}$ gives

$$\mathbf{f}^{i(N)} = \sum_{j=1}^{N} \bar{\boldsymbol{\tau}}_N^{(i,j)} \cdot \exp[-i\mathbf{k}_{\mathrm{inc}} \cdot \mathbf{r}_j] \cdot \mathbf{a}. \tag{19}$$

Recently, we presented complete analytical formulations of the optical parameters using this phase shift formalism applied to the N-centered T-matrix concept [18,29]. We would like to stress the fact that the terminology, numerical convergence, should be handled with caution when it is referred to a recursive algorithm. Indeed examining the fundamental relations of the RCTMA, one can note that they do not involve any convergence parameters as for an iterative technique.

5. Numerical validation

We present now a comparative study of the RCTMA and the GMM formalism developed by Xu. In order to have a study which represents a wide range of different configurations, we choose to present here the 5 following systems: 9 spheres in a plane, 14 spheres in a pyramidal configurations, 10 spheres in a linear array, 9 spheres in a cubic centered structure, and 13 spheres in a compact cluster. The complex indices of refraction of the particles are different for each system, but are the same for each of the particles in each configuration. The index of refraction of the surrounding medium is real and kept at $n_0 = 1.0$.

The size parameter of all the spheres is equal to 2 throughout the study. Following the Wiscombe criterion, the corresponding truncation for the expansion of the electromagnetic fields is $n_{\max}=9$. For each configurations, we calculated the average total cross-section. We also have evaluated the asymmetry parameters, the coefficients S_{11} and S_{22} of the amplitude scattering matrix and the total cross-sections when the direction of the incident wave vector is parallel to the Oz-axis. Each optical parameter is evaluated independently of the others. The sizes and exact positions of each sphere in the different systems are given in Appendix B. Figs. 1–6 show the square modulus of the amplitude scattering coefficients S_{11} and S_{22} in a log scale, as a function of polar angle θ_s, where $0^\circ \leqslant \theta_s \leqslant 180^\circ$ while the azimuth angle ϕ_s is kept equal to zero. The solid line represents the numerical results

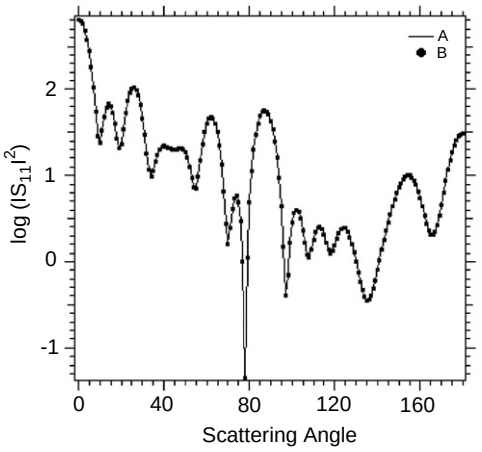

Fig. 1. Configuration C_1: 9 spheres in a plane. Square module of the amplitude scattering matrix element S_{11}. (A) Solid line, GMM. (B) Dotted line, RCTMA.

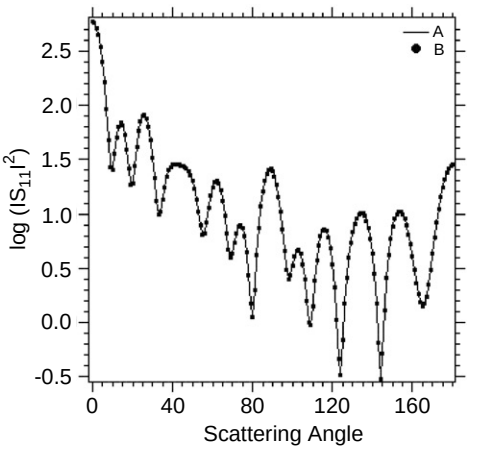

Fig. 2. Configuration C_1: 9 spheres in a plane. Square module of the amplitude scattering matrix element S_{22}. (A) Solid line, GMM. (B) Dotted line, RCTMA.

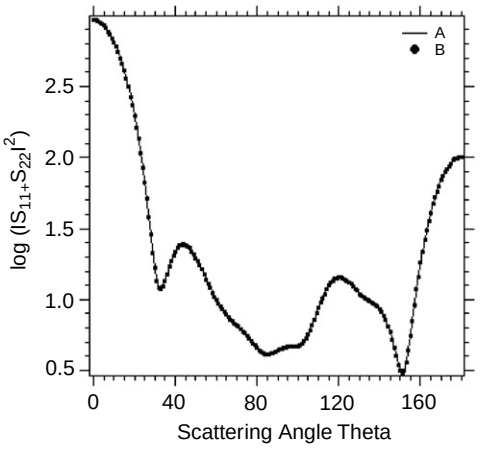

Fig. 3. Configuration C_2: 14 spheres in a pyramidal configuration. Half sum of the square module of the amplitude scattering matrix element S_{11} and S_{22}. (A) Dotted line, GMM. (B) Dots, RCTMA.

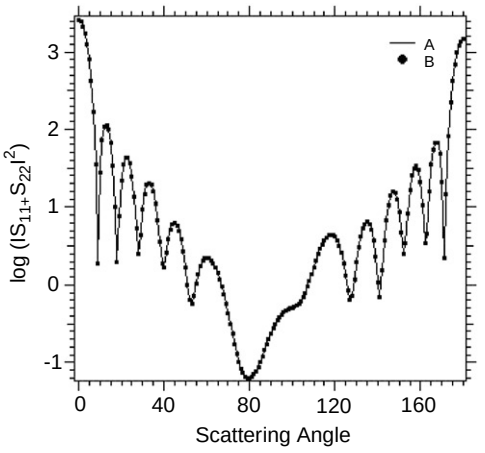

Fig. 4. Configuration C_3: 10 spheres in line. Half sum of the square module of the amplitude scattering matrix element S_{11} and S_{22}. (A) Dotted line, GMM. (B) Dotted line, RCTMA.

calculated from GMM, while the points represent those from the RCTMA. One can see the perfect match between both algorithms for every configuration.

The total scattering cross-sections and the asymmetry parameter for a fixed orientation of the incident wave vector parallel to the *Oz*-axis are given in Tables 1–4 for both polarizations, while the average total cross sections are showed in Tables 5 and 6. In this case, one can also see the great agreement between both algorithms.

In order to show the differences between the RATMA and RCTMA, Fig. 7 represents the scattering cross-section of four dielectric spheres as a function of their size. The particles are placed on a

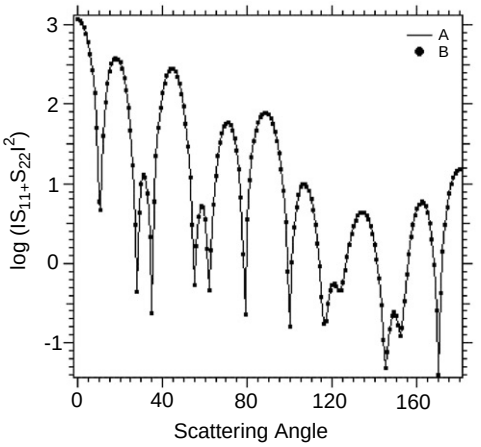

Fig. 5. Configuration C_4: 9 spheres in cubic center configuration. Half sum of the square module of the amplitude scattering matrix element S_{11} and S_{22}. (A) Solid line, GMM. (B) Dotted line, RCTMA.

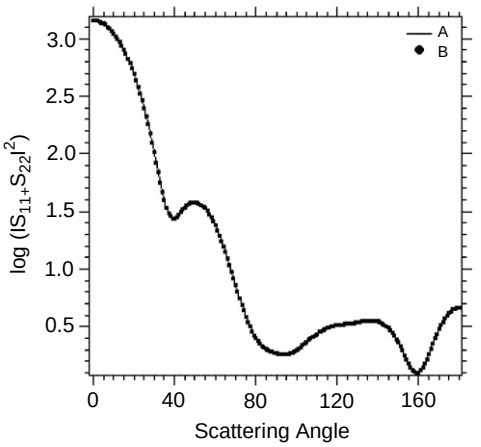

Fig. 6. Configuration C_5: 13 spheres in a compact configuration. Half sum of the square module of the amplitude scattering matrix element S_{11} and S_{22}. (A) Solid line, GMM. (B) Dotted line, RCTMA.

Table 1
GMM formalism, TE polarization of the incident electric field: Total cross-sections (μm^2) and asymmetry parameter (dimensionless) of the five different configurations under study

	C_{ext}^{TE}	C_{sca}^{TE}	C_{abs}^{TE}	g^{TE}
C_1	66.214	51.785	14.432	0.55590
C_2	631.02	631.03	0.0	0.49086
C_3	475.84	475.85	0.0	0.046877
C_4	625.62	425.59	200.02	0.63630
C_5	851.34	814.10	37.231	0.83835

Table 2
RCTMA formalism,TE polarization of the incident electric field: Total cross-sections (μm^2) and asymmetry parameter (dimensionless) of the five different configurations under study

	C_{ext}^{TE}	C_{sca}^{TE}	C_{abs}^{TE}	g^{TE}
C_1	66.2173	51.7851	14.4322	0.555904
C_2	631.004	631.004	0.0	0.490924
C_3	475.846	475.846	0.0	0.0468746
C_4	625.617	425.595	200.022	0.636298
C_5	851.337	814.105	37.2316	0.838347

Table 3
GMM formalism, TM polarization of the incident electric field: Total cross-sections (μm^2) and asymmetry parameter (dimensionless) of the five different configurations under study

	C_{ext}^{TM}	C_{sca}^{TM}	C_{abs}^{TM}	g^{TM}
C_1	69.860	54.893	14.967	0.55042
C_2	632.55	632.55	0.0	0.39534
C_3	1353.1	1353.1	0.0	0.11495
C_4	625.62	425.59	200.02	0.63630
C_5	835.62	798.51	37.111	0.82346

Table 4
RCTMA formalism,TM polarization of the incident electric field: Total cross-sections (μm^2) and asymmetry parameter (dimensionless) of the five different configurations under study

	C_{ext}^{TM}	C_{sca}^{TM}	C_{abs}^{TM}	g^{TM}
C_1	69.8604	54.8931	14.9674	0.550417
C_2	632.567	632.567	0.0	0.395404
C_3	1353.09	1353.09	0.0	0.114949
C_4	625.617	425.595	200.022	0.636298
C_5	835.620	798.509	371.106	0.823457

Table 5
GMM formalism: Total average cross-sections (μm^2) of the five different configurations under study

	$\langle C_{ext} \rangle$	$\langle C_{sca} \rangle$	$\langle C_{abs} \rangle$
C_1	54.6033	43.4492	11.1541
C_2	616.156	616.156	0.0
C_3	744.372	744.372	0.0
C_4	560.972	373.810	187.62
C_5	835.265	797.615	37.65

Table 6
RCTMA formalism: Total average cross-sections (μm^2) of the five different configurations under study

	$\langle C_{ext} \rangle$	$\langle C_{sca} \rangle$	$\langle C_{abs} \rangle$
C_1	54.6034	43.4492	11.1542
C_2	615.851	615.850	0.0
C_3	744.359	744.359	0.0
C_4	560.973	373.811	187.62
C_5	835.371	797.823	37.549

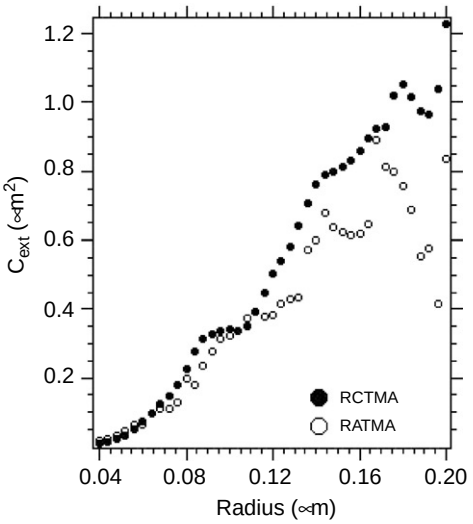

Fig. 7. Scattering cross-sections of four dielectric spheres in a tetrahedric configuration as a function of their size. The incident wave vector is parallel to the Oz axis and the electric field has a TE polarization. The wavelength is 0.546 μm, $n_s^i = 2.8$ and $n_0 = 1.5$. Black circles RCTMA. White circles RATMA.

tetrahedral configuration, and the incident wave vector is parallel to the Oz-axis. The wavelength is 0.546 μm while the indices of refraction of the particles and surrounding medium are $n_s^i = 2.8$ and $n_0 = 1.5$, respectively. One can see from Fig. 7, that both algorithms give relatively close results for very small particles. However, when the size of the spheres increases, one can notice the numerical instability of the RATMA.

6. Conclusion

We presented a new set of recursive relations in order to solve the multiple T-matrices of a system composed of N dielectric spheres in interaction. This new method is based on the N-centered T-matrix concept. We showed that its numerical stability arises from the fact that it only involves translation matrices with a cut-off related to the size parameter of the particles, whereas the RTMA and RATMA use translation matrices that have their dimension linked to the size of the entire system.

This gain in numerical stability is however associated with an increase of the total number of matrices that have to be evaluated. While this number is proportional to N for the RTMA, it is now proportional to N^2 for the RCTMA. We have validated the stability of the algorithm by comparing its numerical result with those obtained from the Generalized Multiparticle Mie formalism on various complex systems. We showed that the recursive procedure gives numerical result in very good agreement with the GMM formalism. For a fixed incident field, iterative techniques are apparently the faster of the two algorithms because they do not involve a matrix inversion. However, due to its recursive nature, the RCTMA does not depend on convergence's parameters.

Acknowledgements

The authors would like to thank Yu Lin Xu for providing the numerical results of the GMM formalism and Eduardo Nahmad for his encouragement.

Appendix A. Translation theorem

The expressions of the translational theorem for spherical wave functions are:

$$Rg\{\boldsymbol{\Psi}^{(3)t}(k_0\,|\mathbf{r}-\mathbf{r}_i|)\} = Rg\{\boldsymbol{\Psi}^{(3)t}(k_0\,|\mathbf{r}-\mathbf{r}_k|)\}\cdot\bar{\mathbf{J}}^{(k,i)} \quad \forall r_{ik}, \tag{A.1}$$

$$\boldsymbol{\Psi}^{(3)t}(k_0\,|\mathbf{r}-\mathbf{r}_i|) = Rg\{\boldsymbol{\Psi}^{(3)t}(k_0\,|\mathbf{r}-\mathbf{r}_k|)\}\cdot\bar{\mathbf{H}}^{(k,i)}, \quad r < r_{ik}, \tag{A.2}$$

$$\boldsymbol{\Psi}^{(3)t}(k_0\,|\mathbf{r}-\mathbf{r}_i|) = \boldsymbol{\Psi}^{(3)t}(k_0\,|\mathbf{r}-\mathbf{r}_k|)\cdot\bar{\mathbf{J}}^{(k,i)} \quad r > r_{ik}, \tag{A.3}$$

where $\bar{\mathbf{J}}^{(k,i)}$ and $\bar{\mathbf{H}}^{(k,i)}$ are the translational matrices which can be written as

$$\bar{\mathbf{J}}^{(k,i)} = \begin{bmatrix} Rg\{A_{nm}^{\nu\mu(q)}\} & Rg\{B_{nm}^{\nu\mu(q)}\} \\ Rg\{B_{nm}^{\nu\mu(q)}\} & Rg\{A_{nm}^{\nu\mu(q)}\} \end{bmatrix} \quad \text{and} \quad \bar{\mathbf{H}}^{(k,i)} = \begin{bmatrix} A_{nm}^{\nu\mu(q)} & B_{nm}^{\nu\mu(q)} \\ B_{nm}^{\nu\mu(q)} & A_{nm}^{\nu\mu(q)} \end{bmatrix}. \tag{A.4}$$

The $A_{nm}^{\nu\mu(q)}$ and $B_{nm}^{\nu\mu(q)}$ are the translation coefficients needed for the transformation from the ith to the kth coordinate system. They depend on the position vector $\mathbf{r}_{ki}$ between the two spheres, and the amplitude of the wave-vector of the medium in which they are imbedded.

Appendix B. Description of the systems

The characteristics of the five different configurations are given in the following vector form: $\{i, X_i, Y_i, Z_i, a_i, Re(n_s^i), Im(n_s^i)\}$ where the subscript i represents the ith sphere in the system and X_i, Y_i and Z_i are its cartesien coordinate, a_i is the radius, $Re(n_s^i)$ and $Im(n_s^i)$ the real and imaginary part of its complex index of refraction. The index of the surrounding medium is real and kept constant at n_0=1.0 for all configurations.

Configuration 1 (C_1): 9 dielectric spheres in a plane. The wavelength of the incident wave is $\lambda_0=\pi$ and the characteristics of each sphere are given by $\{1, 0.0, 0.0, 0.0, 1.0, 2.516, 0.12\}$; {2,0.0,0.0,6.4, 1.0, 1.625,0.015}; {3,0.0,0.0,− 6.4,1.0,1.625,0.015}; {4,6.4,0.0,0.0,1.0,1.625,0.015}; {5,− 6.4,0.0, 0.0, 1.0, 1.625,0.015}; {6,− 6.4,0.0,6.4,1.0,1.3,0.08}; {7,− 6.4,0.0,− 6.4,1.0,1.3,0.08}; {8,6.4, 0.0, 6.4, 1.0,1.3,0.08}; {9,6.4,0.0,− 6.4,1.0,1.3,0.08}

Configuration 2 (C_2): 14 dielectric spheres in a pyramidal configuration. The wavelength of the incident wave is $\lambda_0 = 10.053$ and the characteristics of each sphere are given by: {1,0.0,0.0, 0.0,3.2,2.8,0.0}; {2,0.0,0.0,6.4,3.2,2.8,0.0}; {3,0.0,0.0,−6.4,3.2,2.8,0.0}; {4,6.4,0.0,0.0,3.2,2.8,0.0}; {5,−6.4,0.0,0.0,3.2,2.8,0.0}; {6,3.2,4.5255,3.2,3.2,2.8,0.0}; {7,−3.2,4.5255,−3.2,3.2,2.8,0.0}; {8,3.2, 4.5255, − 3.2,3.2,2.8,0.0}; {9,− 3.2,4.5255,3.2,3.2,2.8,0.0}; {10,6.4,0.0,6.4,3.2,2.8,0.0}; {11,− 6.4, 0.0,− 6.4,3.2,2.8,0.0}; {12,− 6.4,0.0,6.4,3.2,2.8,0.0}; {13,6.4,0.0,− 6.4,3.2,2.8,0.0}; {14,0.0,9.051, 0.0,3.2,2.8,0.0}.

Configuration 3 (C_3): 10 dielectric spheres in a line. The wavelength of the incident wave is $\lambda_0 = 10.053$ and the characteristics of each sphere are given by: {1,3.2,0.0,0.0, 3.2,2.8,0.0}; {2,−3.2,0.0,0.0,3.2,2.8,0.0}; {3,9.6,0.0,0.0,3.2,2.8,0.0}; {4,−9.6,0.0,0.0,3.2,2.8,0.0}; {5,16.0,0.0,0.0,3.2,2.8,0.0}; {6,−16.0,0.0,0.0,3.2,2.8,0.0}; {7,22.4,0.0,0.0,3.2,2.8,0.0}; {8,−22.4,0.0, 0.0,3.2,2.8,0.0}; {9,28.8,0.0,0.0,3.2,2.8,0.0}; {10,−28.8,0.0,0.0,3.2,2.8,0.0}.

Configuration 4 (C_4): 9 dielectric spheres cubic center structure. The wavelength of the incident wave is $\lambda_0 = 10.053$ and the characteristics of each sphere are given by: {1,0.0,0.0,0.0,3.2,1.5,0.1}; {2,−15.0,−15.0,−15.0,3.2,1.5,0.1}; {3,−15.0,15.0,−15.0,3.2,1.5,0.1}; {4,15.0,15.0, −15.0, 3.2, 1.5, 0.1}; {5,15.0,−15.0,−15.0,3.2,1.5,0.1}; {6,−15.0,−15.0,15.0,3.2,1.5,0.1}; {7,−15.0,15.0, 15.0,3.2, 1.5,0.1}; {8,15.0,15.0,15.0,3.2,1.5,0.1}; {9,15.0,−15.0,15.0,3.2,1.5,0.1}.

Configuration 5 (C_5): 13 dielectric spheres in a compact structure. The wavelength of the incident wave is $\lambda_0 = 10.053$ and the characteristics of each sphere are given by: {1,0.0,0.0,0.0,3.2,1.5,0.01}; {2,5.4443,−3.36471,0.0,3.2,1.5,0.01}; {3,0.0,5.4443,−3.36471,3.2,1.5,0.01}; {4,−3.36471,0.0, 5.4443,3.2,1.5,0.01}; {5,0.0, −5.4443,−3.36471,3.2,1.5,0.01}; {6,3.36471,0.0,5.4443,3.2,1.5,0.01}; {7,−5.4443,3.36471,0.0,3.2,1.5,0.01}; {8,0.0,5.4443,3.36471,3.2,1.5,0.01}; {9,3.36471,0.0,−5.4443, 3.2,1.5,0.01}; {10,−5.4443,−3.36471,0.0,3.2,1.5,0.01}; {11,5.4443,3.36471,0.0,3.2,1.5,0.01}; {12, 0.0,−5.4443,3.36471,3.2,1.5,0.01}; {13,−3.36471,0.0,−5.4443,3.2,1.5,0.01}

References

[1] Frisch U. Ann Astrophys 1966;29:645–82;
Frisch U. Ann Astrophys 1966;30:565–601.

[2] Beard CI, Kays TH, Twersky V. Scattering by random distribution of spheres vs. concentration. IEEE Trans Antennas Propag 1967;15(1):99–118.

[3] Chandrasekhar S. Radiative transfer, New York: Dover Publications, 1960.

[4] Ishimaru A. Wave propagation and scattering in random media, vols. 1 and 2. New York: Academic Press, 1978.

[5] Tsang L, Kong J, Shin R. Theory of microwave remote sensing. New York: Wiley, 1985.

[6] Cartigny JD, Yamada Y, Tien CL. Radiative transfer with dependent scattering by particles: part I—theoretical investigation. ASME J Heat Transfer 1986;108:608–13.

[7] Kumar S, Tien CL. Dependent absorption and extinction of radiation by small particles. Trans ASME 1990;112: 178–85.

[8] Watermann P. Symmetry unitary and geometry in electromagnetic scattering. Phys Rev D 1971;3(4):825–39.

[9] Borghese F, Denti P, Saija R, Toscano G. Multiple electromagnetic scattering from a cluster of spheres I: theory. Aerosol Sci Technol 1984;4:227–35.

[10] Fuller KA. Consummate solution to the problem of classical electromagnetic scattering by an ensemble of spheres I: linear chains. Opt Lett 1988;13(2):90–2.

[11] Hamid A. Electromagnetic scattering by an arbitrary configuration of dielectric spheres. Can J Phys 1990;68: 1419–28.

[12] Chew W. Waves and fields in inhomogeneous media. IEEE PRESS Series on Electromagnetic Waves, 1990.

[13] Mackowski D. Calculation of total cross sections of multiple-sphere clusters. J Opt Soc Am A 1994;11(11): 2851–61.

[14] Tzeng Y, Fung A. T-matrix approach to multiple scattering of EM waves from N-spheres. J Electromagn Waves Appl 1994;8(1):61–84.

[15] Mishchenko MI, Mackowski DW. Scattering of light by bispheres with touching and separated components. Appl Opt 1995;34(21):4589–99.

[16] Xu Y. Electromagnetic scattering by an aggregate of spheres. Appl Opt 1995;34(21):4573–88.

[17] Auger JC, Stout B, Barrera RG. Scattering properties of rutile pigments located eccentrically within microvoids. JQSRT 2001;70:675–95.

[18] Stout B, Auger JC, Lafait J. A transfer matrix approach to local field calculations in multiple scattering problems. J Mod Opt 2002;49(13):2129–52.
[19] Mackowski D, Mishchenko M. Calculation of the *T*-matrix and the scattering matrix for ensembles of spheres. J Opt Soc Am A 1996;13(11):2266–78.
[20] Xu YL, Gustafson BAS. A generalized multiparticle Mie-solution: further experimental verification. JQSRT 2001;70:395–419.
[21] Bohren CF, Huffman DR. Absorption and scattering of light by small particles. New York: Wiley-Interscience Publication, 1983.
[22] Stein S. Addition theorems for spherical wave functions. Q Appl Math 1961;19(1):15–24.
[23] Cohen-Tannoudji, Diu B, Laloe F. Mecanique quantique vol. 2. Paris: Hermann Editeur des Sciences et des Arts, 1973.
[24] Wiscombe W. Improve Mie scattering algorithms. Appl Opt 1980;19(9):1505–9.
[25] Fuller K. Scattering and absorption cross sections of compounded spheres I: theory for external aggregation. J Opt Soc Am A 1994;11(12):3251–60.
[26] Liang C, Lo YT. Scattering by two spheres. Radio Sci 1967;2(12):1481–95.
[27] Bruning J, Lo YT. Multiple scattering of EM waves by spheres part I-multipole expansion and ray-optical solutions. IEEE Trans Antennas Propag 1971;19:378–90.
[28] Bruning J, Lo YT. Multiple scattering of EM waves by spheres part II-numerical and experimental results. IEEE Trans Antennas Propag 1971;19:391–400.
[29] Stout B, Auger JC, Lafait J. Individual and aggregate scattering matrices and cross-sections: conservation laws and reciprocity. J Mod Opt 2001;48(14):2105–28.